AGU100 ADVANCING EARTH AND SPACE SCIENCE

Geophysical Research Letters

RESEARCH LETTER
10.1029/2018GL081500

Key Points:
- The solar wind dynamic pressure fluctuations excited the fundamental toroidal standing Alfvén waves in the dayside magnetosphere
- The regular toroidal pulsations simultaneously modulated the whistler-mode chorus, exohiss, and magnetosonic emissions from 50 Hz to 5 kHz
- No modulation signatures of background parameters and resonant particles for these whistler-mode emissions were observable near the equator

Supporting Information:
- Supporting Information S1

Correspondence to:
Z. Su,
szpe@mail.ustc.edu.cn

Citation:
Liu, N., Su, Z., Gao, Z., Zheng, H., Wang, Y., & Wang, S. (2019). Magnetospheric chorus, exohiss, and magnetosonic emissions simultaneously modulated by fundamental toroidal standing Alfvén waves following solar wind dynamic pressure fluctuations. *Geophysical Research Letters*, *46*, 1900–1910. https://doi.org/10.1029/2018GL081500

Received 30 NOV 2018
Accepted 5 FEB 2019
Accepted article online 8 FEB 2019
Published online 15 FEB 2019

Magnetospheric Chorus, Exohiss, and Magnetosonic Emissions Simultaneously Modulated by Fundamental Toroidal Standing Alfvén Waves Following Solar Wind Dynamic Pressure Fluctuations

Nigang Liu[1,2,3,4], Zhenpeng Su[1,2,3], Zhonglei Gao[5,6], Huinan Zheng[1,2,3], Yuming Wang[1,2,3], and Shui Wang[1,2,3]

[1]CAS Key Laboratory of Geospace Environment, Department of Geophysics and Planetary Sciences, University of Science and Technology of China, Hefei, China, [2]Collaborative Innovation Center of Astronautical Science and Technology, University of Science and Technology of China, Hefei, China, [3]CAS Center for Excellence in Comparative Planetology, Hefei, China, [4]Mengcheng National Geophysical Observatory, School of Earth and Space Sciences, University of Science and Technology of China, Hefei, China, [5]Institute of Space Science and Applied Technology, Harbin Institute of Technology, Shenzhen, China, [6]School of Physics and Electronic Sciences, Changsha University of Science and Technology, Changsha, China

Abstract Magnetospheric quasiperiodic whistler-mode emissions have long been considered a consequence of the relaxation oscillation or the compressional ultralow-frequency wave modulation. Here we experimentally demonstrate that the whistler-mode chorus, exohiss, and magnetosonic emissions can be effectively modulated by the toroidal ultralow-frequency waves. On 04 August 2017, the solar wind dynamic pressure fluctuations excited the fundamental toroidal standing Alfvén waves in the dayside magnetosphere. These regular toroidal pulsations displayed the approximately same periods as the power variations of the whistler-mode emissions from 50 Hz to 5 kHz. Along with the decay of the toroidal pulsations, the quasiperiodic feature of these whistler-mode emissions gradually became indistinct. However, no modulation signatures of background parameters and resonant particles for the whistler-mode emissions were observable near the equator, and the exact cause for this phenomenon remains to be elucidated.

Plain Language Summary Whistler-mode emissions contribute significantly to the Van Allen radiation belt electron dynamics, and their power can exhibit quasiperiodic variations on a timescale of tens of seconds to several minutes in the dayside magnetosphere. Since the 1960s, the quasiperiodic whistler-mode emissions have been considered a consequence of the relaxation oscillation or the compressional ultralow-frequency wave modulation. Using the Van Allen Probes data, we reveal here new physical mechanism for the quasiperiodic whistler-mode emissions: The solar wind dynamic pressure fluctuations trigger the magnetospheric fundamental toroidal standing Alfvén waves and then modulate the whistler-mode chorus, exohiss, and magnetosonic emissions from 50 Hz to 5 kHz. Further investigation of this unexpected phenomenon may deepen our understanding of the growth and propagation of whistler-mode emissions and facilitate the radiation belt model developments.

1. Introduction

Chorus, hiss, and magnetosonic emissions are whistler-mode emissions observed commonly in the inner magnetosphere (Burtis & Helliwell, 1975; Falkowski et al., 2017; Gurnett, 1976; Russell et al., 1969, 1970; Thorne et al., 1973; Tsurutani & Smith, 1974, 1977; Tsurutani et al., 2014, 2009), which have been frequently invoked to explain the complex dynamics of the Van Allen radiation belt electrons (Horne & Thorne, 1998; Shprits, 2009; Summers et al., 1998; Thorne, 2010). These whistler-mode emissions are highly organized by the plasmapause location (Malaspina et al., 2016): Chorus and exohiss are restricted outside the plasmasphere (W. Li et al., 2009; Meredith et al., 2001; Zhu et al., 2015); plasmaspheric hiss is trapped in the plasmasphere (Hayakawa & Sazhin, 1992; Meredith et al., 2004; Tsurutani et al., 2015, 2018; Su et al., 2018a, 2018b); magnetosonic emissions occur more frequently outside than inside the plasmasphere (Kim & Chen, 2016; Ma et al., 2013; Shprits et al., 2013). Their free energies are ultimately provided by the anisotropic hot electrons (Bortnik et al., 2008; Burtis & Helliwell, 1975; Thorne et al., 1979; Tsurutani et al., 1979) or the velocity ring-distributed hot protons (e.g., Boardsen et al., 1992; Gulelmi et al., 1975; Perraut et al., 1982), but the detailed generation processes remain to be fully understood.

In the dayside magnetosphere, the whistler-mode emissions often consist of repeated noise bursts with a lifetime of tens of seconds to several minutes (Carson et al., 1965; Helliwell, 1965). To explain these quasiperiodic emissions, two classes of physical scenarios have been proposed. One envisions the relaxation oscillation of plasma instabilities (Davidson, 1979; Pasmanik, Demekhov, et al., 2004; Pasmanik, Titova, et al., 2004; Trakhtengerts, 1995): (1) the waves grow and resonantly scatter the source particles; (2) when the source distributions are sufficiently relaxed, the wave instabilities are halted; (3) as the fresh particles drift into the source region, the wave instabilities are restarted; (4) the interplay between resonant instabilities and external sources leads to a cyclic variation of the wave power. The other involves the modulation of wave instabilities by the accompanied ultralow-frequency (ULF) waves (Helliwell, 1965; McPherron et al., 1968; Sato & Fukunishi, 1981; Sato et al., 1974): (1) the ULF pulsations modulate the background parameters and the resonant particle distributions; (2) the wave instabilities are cyclically turned on and off. For the former scenario, few observational evidences (Titova et al., 2015) have been provided along with the theoretical and numerical progresses (Davidson, 1986; Demekhov & Trakhtengerts, 1994). In contrast, there is evidence both for and against the latter scenario. Although the ULF pulsations were found to substantially modulate the linear growth rates of whistler-mode emissions in several events (W. Li et al., 2011; Manninen et al., 2010), there are still the quasiperiodic whistler-mode emissions occurring without the observable ULF pulsations (Boardsen et al., 2014; Kitamura et al., 1969; Němec et al., 2014; Sato et al., 1974; Titova et al., 2015; Tsurutani & Smith, 1974) or with the ULF pulsations of the essentially different periods (Němec et al., 2015). Particularly, previous theoretical (e.g., Coroniti & Kennel, 1970; Kimura, 1974; Watt et al., 2011) and observational (e.g., Němec et al., 2014; Sato & Fukunishi, 1981; Tixier & Cornilleau-Wehrlin, 1986) works have focused on the compressional ULF wave modulation, and the potential contributions of the poloidal and toroidal ULF pulsations have long been ignored or even denied (Sato & Kokubun, 1980). Recently, by analyzing magnetospheric waves following a substorm injection, Jaynes et al. (2015) suggested the modulation of chorus emissions by a combination of toroidal and poloidal ULF waves. However, in the event reported by Jaynes et al. (2015), the toroidal and poloidal ULF waves (with a period of ∼2 min) occurred with roughly twice the periodicity as the chorus power variation (with a period of ∼45 s to 1 min), different from the previous one-to-one correlation between the compressional ULF waves and the chorus power variation (e.g., W. Li et al., 2011).

In this letter, we show the surprising observations by the Van Allen Probes (Mauk et al., 2013) of the magnetospheric chorus, exohiss, and magnetosonic emissions simultaneously modulated by the fundamental toroidal standing Alfvén waves following the solar wind dynamic pressure fluctuations. Our observations clearly demonstrate the importance of toroidal ULF pulsations in the generation of quasiperiodic whistler-mode emissions over a broad frequency range.

2. Data and Method

In 2012, the National Aeronautics and Space Administration (NASA) launched the Van Allen Probes mission to explore the fundamental physics of the Earth's radiation belts (Mauk et al., 2013). Here we use the data from the Electric and Magnetic Field Instrument and Integrated Science (EMFISIS) suite (Kletzing et al., 2013), the Electric Field and Waves (EFW) instrument (Wygant et al., 2013), and the Energetic Particle, Composition, and Thermal Plasma (ECT) suite (Spence et al., 2013) on this mission. The EMFISIS suite contains the triaxial fluxgate magnetometer, the Waveform Receiver and the High Frequency Receiver. The EMFISIS suite and the EFW instrument together measure direct current (DC) and alternating current (AC) electromagnetic fields. The ECT suite consists of the Helium Oxygen Proton Electron Mass Spectrometer (Funsten et al., 2013), the Magnetic Electron Ion Spectrometer (Blake et al., 2013), and the Relativistic Electron Proton Telescope (Baker et al., 2013), which collectively detect electrons and ions with energies from electronvolts to tens of megaelectron volts.

From measurements of the magnetic field and the upper hybrid resonance frequency by the EMFISIS suite, we can determine the local cold electron density (Kurth et al., 2014). The spacecraft potential measurement by the EFW instrument allows an alternative estimation of the cold electron density. Specifically, the electron

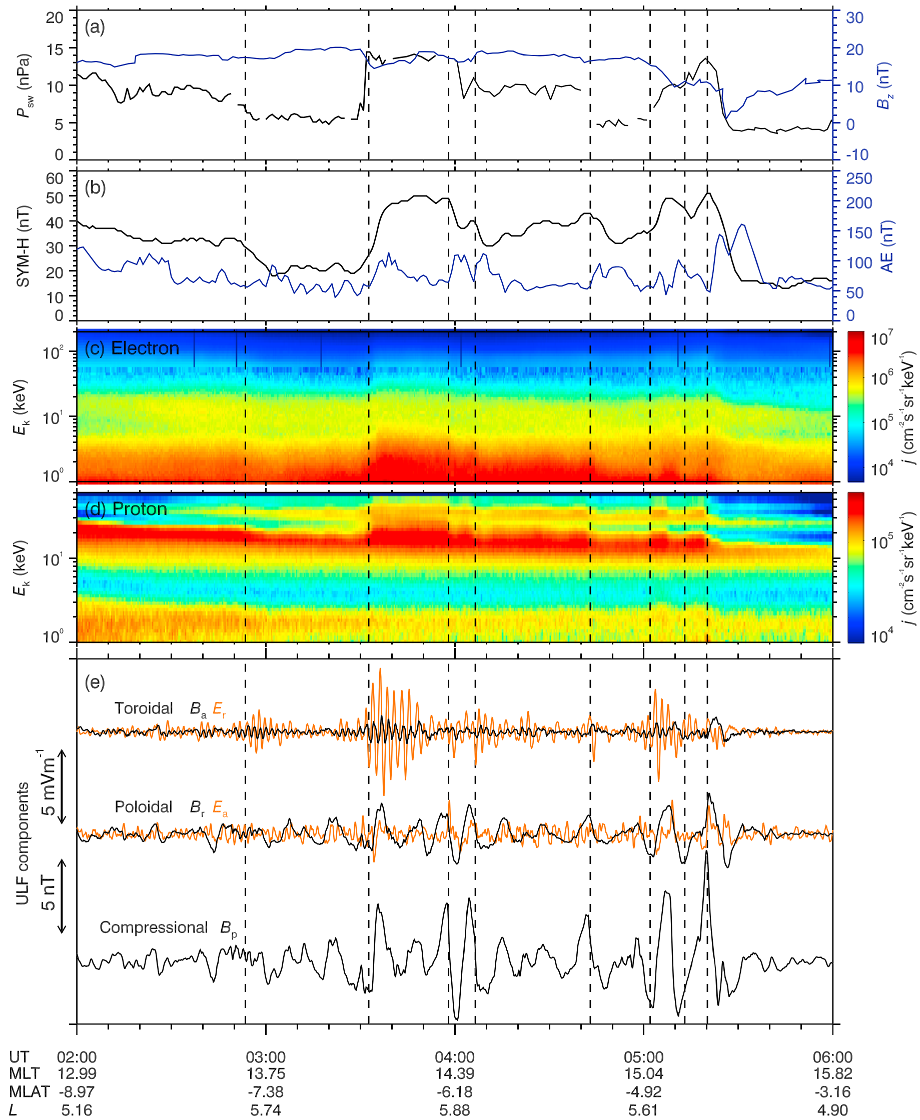

Figure 1. Magnetospheric responses to solar wind disturbances on 04 August 2017: (a) solar wind magnetic filed and dynamic pressure; (b) geomagnetic activity indices; magnetospheric spin-averaged fluxes of hot (c) electrons and (d) protons; (e) magnetospheric toroidal, poloidal, and compressional pulsations. The vertical dashed lines mark the sudden variations in the solar wind dynamic pressure.

density is assumed to be $n_e = a_1 \exp(bx) + a_2 \exp(cx)$, where $x = \overline{(V_1 + V_2)/2}$ is the average of opposing antenna potentials over a spin period (~11 s) of the spacecraft, and a_1, a_2, b, and c are constants determined by fitting to the density data from the EMFISIS suite. We use the TS04 package (Tsyganenko & Sitnov, 2005) to model the ratio of the local magnetic field to the equatorial field. For ULF pulsations, only the two electric components in the spin plane of the satellite are available, and we derive the third component along the spin axis from the assumption $\mathbf{E} \cdot \mathbf{B} = 0$. Note that the angle between satellite spin plane and the magnetic field ranged from 40° to 60° during this specific event. We project the ULF pulsations on the mean field aligned coordinate system (with the p axis along the 1,000-s running averaged magnetic field, the a axis along the cross product of the p axis and the satellite position vector, and the r axis completing the triad) and then apply a band-pass filter (a 20-s running average minus a 500-s running average) on the signals to reduce the noise. These ULF signals are classified into toroidal (E_r and B_a), poloidal (E_a and B_r), and compressional (B_p) components, respectively. For whistler-mode emissions, we estimate the wave vector directions and the magnetic field polarizations by applying the singular value decomposition technique (Santolík et al., 2002,

10.1029/2018GL081500

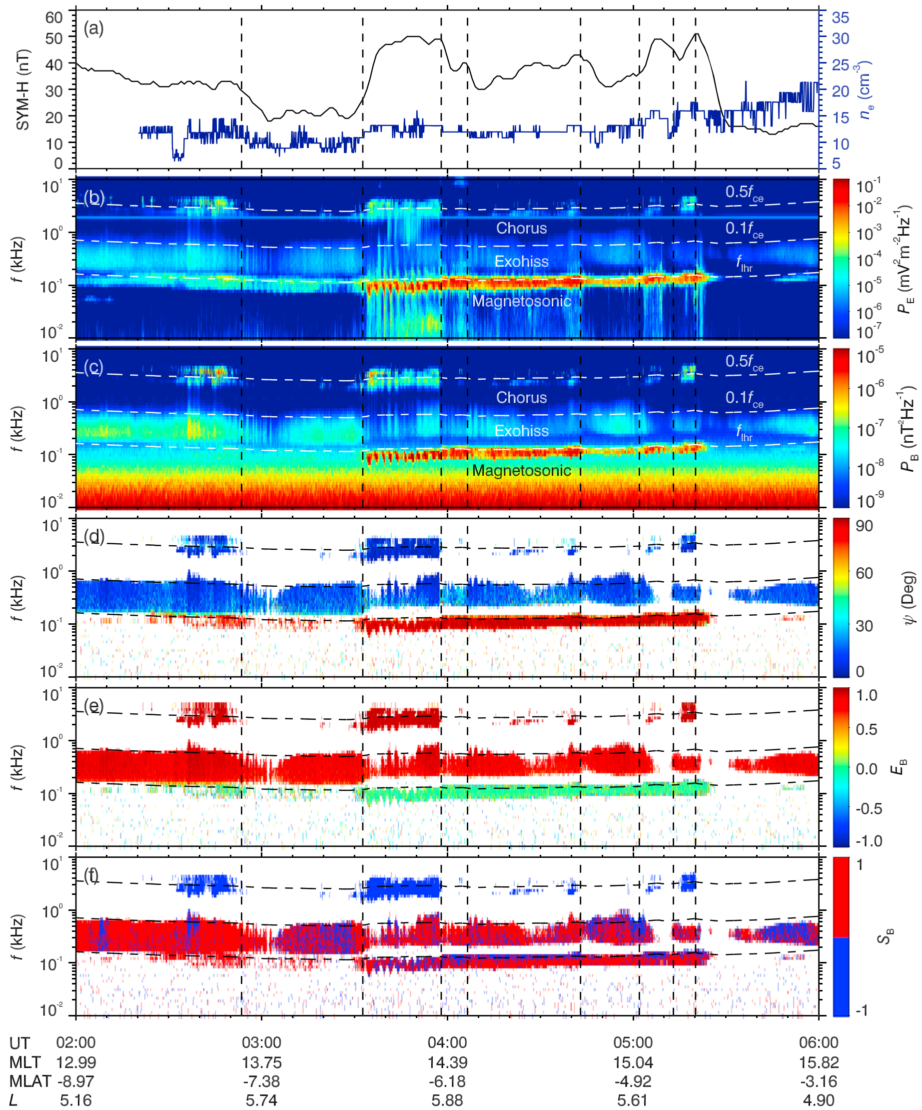

Figure 2. Magnetospheric responses to solar wind disturbances on 04 August 2017: (a) geomagnetic activity index and cold electron density; magnetospheric wave (b and c) power, (d) normal angle, (e) ellipticity (negative for left hand polarized waves and positive for right-handed ones) and (f) parallel Poynting flux sign (positive for parallel flowing and negative for antiparallel flowing). The vertical dashed lines mark the sudden variations in the solar wind dynamic pressure.

2003) on the wave spectral matrices and calculate the wave Poynting fluxes from the cross-power spectra between components of the electric and magnetic fields (Santolík et al., 2010).

3. Observations

Figures 1 and 2 present an overview of interplanetary conditions, geomagnetic activities, and magnetospheric plasma and waves on 04 August 2017. Under the northward interplanetary magnetic field condition, the magnetosphere was free from both storms (SYM-H > 10 nT) and substorms (AE $<$ 180 nT). In the dayside (12 $<$ |MLT| $<$ 16, MLT = magnetic local time) equatorial (|MLAT|< 8°, MLAT = magnetic latitude) plasmatrough ($L > 5$ and $n_e < 30\,\mathrm{cm}^{-3}$), the Van Allen Probe A observed the magnetospheric responses to the solar wind dynamic pressure fluctuations (marked by vertical dashed lines): the enhancement or reduction of hot particle fluxes, the emergence of ULF pulsations, and the intensification or weakening of whistler-mode emissions. Similar phenomena had been reported in the previous works (e.g., Claudepierre et al., 2010; Falkowski et al., 2017; Fu et al., 2012; Liu, Su, Gao, Reeves, et al., 2017; Liu, Su, Gao, Zheng, et al.,

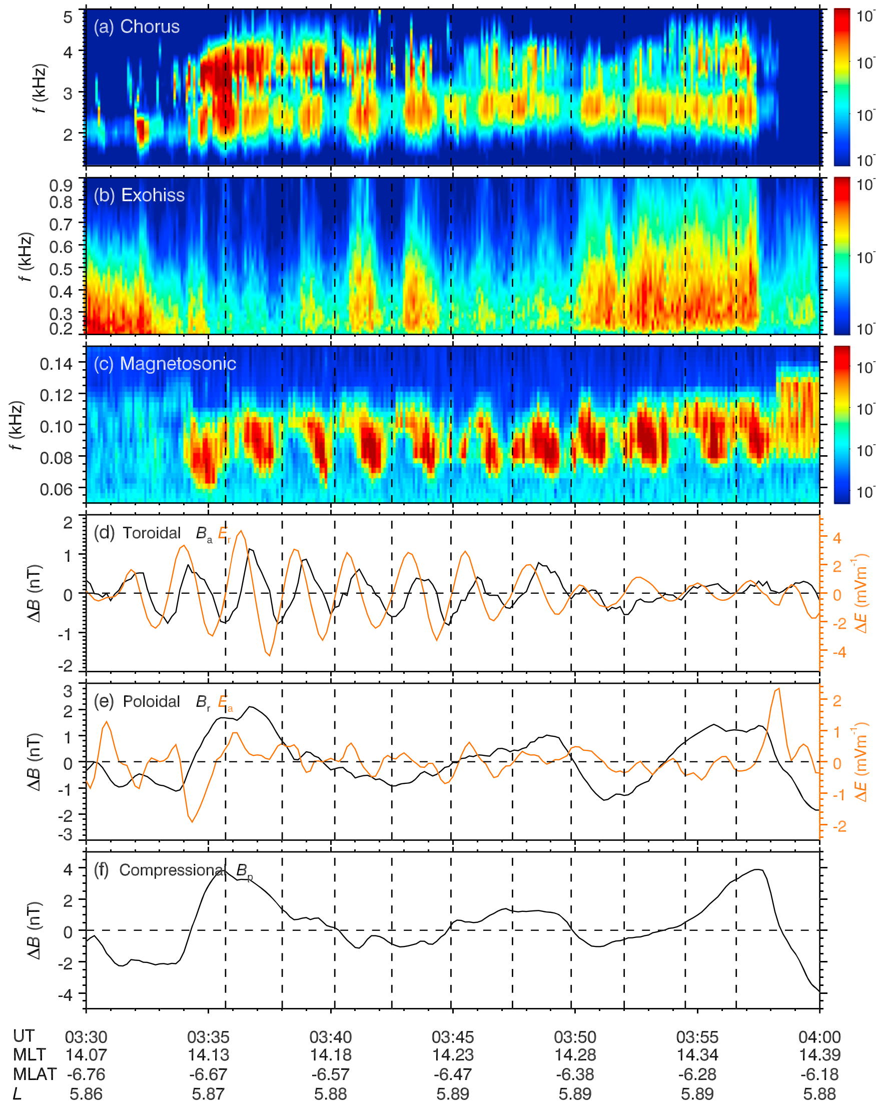

Figure 3. Zoom-in view of magnetospheric waves from 03:30 UT to 04:00 UT: (a) chorus, (b) exohiss, and (c) magnetosonic power; (d) toroidal, (e) poloidal, and (f) compressional pulsations. The overplotted vertical dashed lines help identify the quasiperiodic structures.

2017; Liu et al., 2018b; Su, Zhu, Xiao, Zheng, et al., 2015; Su, Zhu, Xiao, Zong, et al., 2015; Rae et al., 2012). The ULF pulsations were predominant in the toroidal mode of 5–9 mHz with azimuthal magnetic pulsations and radial electric pulsations. Essentially different from the sinusoidal waveforms of the toroidal ULF components, the poloidal and compressional ULF components often behaved in an irregular manner. The whistler-mode emissions can be clearly classified into right circularly polarized chorus (0.3–0.7f_{ce}), right linearly polarized exohiss (0.2–0.8 kHz), and highly elliptically polarized magnetosonic emissions ($< f_{lhr}$). Chorus emissions with a gap at 0.5f_{ce} were excited by the anisotropic hot electrons near the magnetic equator (e.g., W. Li et al., 2009; Su et al., 2014; Tsurutani & Smith, 1977, 1974) and propagated quasi-parallel toward higher latitudes. Exohiss emissions leaked from the high-latitude plasmapause (Bortnik et al., 2008; Gao et al., 2018; Thorne et al., 1973; Zhu et al., 2015) and propagated mainly toward the equator. Magnetosonic emissions were at quasi-perpendicular propagation and closely tracked the lower hybrid frequency (e.g., Tsurutani et al., 2014), which were likely generated by the ring-distributed hot protons (e.g., Gary et al., 2010).

Figure 3 shows a zoom-in view of magnetospheric waves from 03:30 UT to 04:00 UT. At 03:32 UT, the solar wind dynamic pressure enhancement intensified both chorus and magnetosonic emissions but weakened exohiss emissions. As discussed by Liu et al. (2018b), the intensification of chorus and magnetosonic

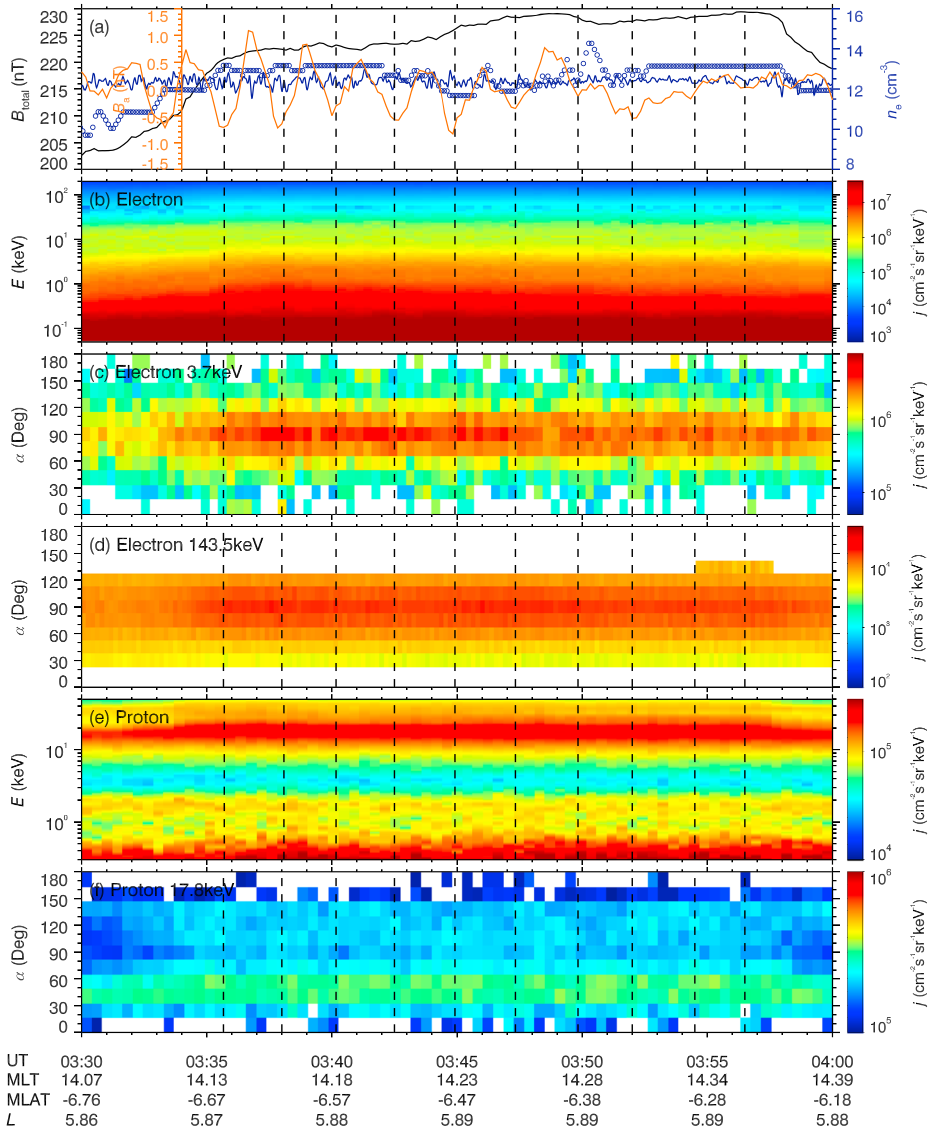

Figure 4. Responses of background parameters and resonant particles of the whistler-mode emissions to toroidal ultralow-frequency pulsations: (a) total magnetic field strength, cold electron density (circles for the Electric and Magnetic Field Instrument and Integrated Science suite and line for the Electric Field and Waves instrument) and azimuthal magnetic perturbation; spin-averaged and differential fluxes of hot (b–d) electrons and (e and f) protons. The vertical dashed lines are exactly the same as those in Figure 3.

emissions probably resulted from the adiabatic acceleration of source particles (Figures 1c and 1d). The weakening of exohiss emission was likely a result of the enhanced Landau damping at high latitudes or the geomagnetic field reconfiguration. During the next ~25 min, all these whistler-mode emissions exhibited the synchronous and quasiperiodic (2–3 min) variations in power. After the solar wind dynamic pressure reduction at 03:58 UT, these quasiperiodic whistler emissions became unobservable. Because the three types of emissions had essentially different origins, their independent relaxation oscillations were difficult to produce the same variation cycle. In contrast to the irregular ULF poloidal and compressional components, the regular toroidal ULF pulsations always exhibited the approximately same periods as the power variations of these whistler-mode emissions. Corresponding to the toroidal ULF pulsations with a decreasing amplitude, the quasiperiodic feature of these whistler-mode emissions gradually became indistinct. Our observations strongly imply the modulation of these whistler-mode emissions from 50 Hz to 5 kHz by the coexisting toroidal ULF pulsations. Clearly, the azimuthal magnetic pulsations leaded the radial electric pulsations by approximately 90° in phase, and near the magnetic equator, the azimuthal magnetic pulsations were quite small (below 2 nT) in contrast to the large radial electric pulsations (up to 4.5 mV/m). The acting toroidal ULF pulsations associated with the solar wind dynamic pressure fluctuations were most likely to be the fundamental standing Alfvén waves (Anderson et al., 1990; Hudson et al., 2004; Takahashi et al., 2006). It should be mentioned that in the time range of interest, the Van Allen Probe B within the duskside plasmasphere observed the concurrence of toroidal, poloidal, and compressional ULF pulsations with small amplitudes and the quasiperiodic plasmaspheric hiss at frequencies greater than ~3 kHz (supporting information Figure S1). However, the ULF pulsations (with periods ~2 min) were unlikely to be responsible for the quasiperiodic variations (~12 s) in the hiss power.

In Figure 4, we analyze the evolution of background parameters and resonant particles for the whistler-mode emissions. The background magnetic field strength and the cold electron density determine the wave dispersion relation, and the resonant particles contribute to growth or decay of the whistler-mode emissions. In contrast to the local generation of chorus and magnetosonic emissions, the source locations of exohiss emissions were likely beyond the orbital coverage of the Van Allen Probes. A plausible scenario is that the chorus emissions at larger radial distances propagate into the plasmasphere, evolve into the plasmaspheric hiss emissions (Bortnik et al., 2008; Falkowski et al., 2017; W. Li et al., 2015; Tsurutani et al., 2015), leak from the dayside high-latitude plasmapause, and finally become the exohiss emissions (Gao et al., 2018; Liu, Su, Gao, Zheng, et al., 2017; Zhu et al., 2015). At the location of Van Allen Probe A, the minimum resonant energies of electrons (Summers et al., 2007) were about 3 keV for chorus at 3 kHz and 120 keV for exohiss at 0.4 kHz, and the growth of magnetosonic emissions was related to the proton rings centered at 17 keV. At 03:32 and 03:58 UT, the magnetic field strength, the cold electron density, and the hot particle fluxes responded promptly to the sudden variations of solar wind dynamic pressure. However, both background parameters and resonant particles exhibited no observable ULF modulation signatures from 03:32 to 03:57 UT. The random fluctuations of the derived density did not correlate with the ULF pulsations, and the modulation signatures of the particle fluxes at the other energy channels were also unobservable (Figures S2–S4). These observations were quite different from the situations in the previous compressional ULF modulation events (e.g., J. Li et al., 2017; W. Li et al., 2011; Xia et al., 2016).

4. Discussions

In the past, the compressional ULF modulation of chorus has been frequently observed both on ground and in space (e.g., Kimura, 1974; W. Li et al., 2011; Manninen et al., 2010; Sato & Fukunishi, 1981; Xia et al., 2016), the modulation of chorus by a combination of the toroidal and poloidal ULF waves has been examined in an event study (Jaynes et al., 2015), no observations have explicitly shown the modulation of exohiss by any ULF modes, and the accompanied compressional ULF pulsations have been found to possess the systematically larger periods than the quasiperiodic magnetosonic emissions (Němec et al., 2015). Our present study clearly demonstrates the toroidal ULF modulation of three types of whistler-mode emissions approximately from 50 Hz to 5 kHz. Particularly, the chorus power variation is found to show a one-to-one correlation with the toroidal ULF waves, different from the previous observations of Jaynes et al. (2015). Such a modulation phenomenon appears to be not rare in the dayside magnetosphere following the solar wind dynamic pressure fluctuations. On the same day as Figure 3, there were also signatures of the toroidal ULF modulation of exohiss and magnetosonic emissions from 02:50 to 03:05 UT (Figure S5) and from 05:00 to 05:20 UT (Figure S6). Compared to the interval of Figure 3, the intervals of Figures S5 and S6 with the weaker ULF pulsations allowed the less obvious quasiperiodic variations in the whistler-mode power. Another interesting feature of Figure 3 is the falling frequency magnetosonic emissions in each cycle, different from the previously reported rising frequency magnetosonic emissions (Boardsen et al., 2014; Fu et al., 2014). These magnetosonic frequency sweep structures might be composed of the non-time-continuous harmonic emission lines along the proton gyrofrequency harmonics in the high-resolution frequency-time spectrogram (Němec et al., 2015; Walker et al., 2016). Note that the magnetosonic harmonic rising and falling frequency emission lines deviating from the proton gyrofrequency harmonics had been reported under the conditions of the substorm proton injection (Su et al., 2017) or the nonlinear wave-wave interactions (Liu et al., 2018a).

For the fundamental standing Alfvén waves, the magnetic field pulsations have a node at the equator (Southwood & Kivelson, 1981). Under the ideal magnetohydrodynamic condition, the density should vary in phase with the magnetic field. When the satellite flies slightly away from the equator, the pulsations of magnetic field and density remain at low level. For the hot electrons with the cyclotron, bounce, and drift frequencies substantially deviating from the observed toroidal wave frequency, their adiabatic oscillations are ignorable corresponding to the tiny (<1%) oscillation of the toroidal ULF magnetic field (Figure 4). To explain the quasiperiodic chorus and exohiss emissions in resonance with hot electrons, we may consider the ULF modulation of the geomagnetic field configuration. For the chorus generated at the equator, both theoretical (Katoh & Omura, 2013; Katoh et al., 2018; Omura et al., 2008) and observational (Keika et al., 2012; Liu, Su, Gao, Zheng, et al., 2017) studies have suggested that the spatial inhomogeneity of the background magnetic field can control the adiabatic force on the resonant electrons and then affect the nonlinear growth process. For the exohiss emissions leaking from the high-latitude plasmapause, their propagation paths and then the near-equatorial power should also depend on the geomagnetic field configuration. As for the hot (10–20 keV) protons, their bounce frequencies in a dipole field are quite close to the toroidal wave frequencies (5–9 mHz), allowing the action of bounce resonance (Southwood & Kivelson, 1981, 1982). There have been observations of the bounce resonance between poloidal ULF pulsations and hot ions in the inner magnetosphere (Yang et al., 2010). By analogy, we can expect the fundamental toroidal standing Alfvén waves to modulate the hot proton distributions and then the magnetosonic power. Probably because of the rapid relaxation by the magnetosonic emissions or the limited detection efficiency of the Van Allen Probes, only small irregular oscillations of these hot proton fluxes (Figure S4) were recorded.

5. Summary

Magnetospheric quasiperiodic whistler-mode emissions were usually considered a consequence of the relaxation oscillation (Davidson, 1986; Demekhov & Trakhtengerts, 1994; Titova et al., 2015) or the compressional ULF modulation (Coroniti & Kennel, 1970; Kimura, 1974; Němec et al., 2014; Sato & Fukunishi, 1981; Tixier & Cornilleau-Wehrlin, 1986; Watt et al., 2011). Recently, Jaynes et al. (2015) suggested the modulation of chorus by a combination of toroidal and poloidal ULF pulsations following the substorm injection. On the basis of the analysis of a rare event where chorus, exohiss, and magnetosonic emissions exhibited the synchronous and quasiperiodic variations in power, we here show that the toroidal ULF pulsations can effectively modulate the whistler-mode emissions over a broad frequency range. On 04 August 2017, the solar wind dynamic pressure fluctuations produced the dayside magnetospheric ULF pulsations predominantly in the fundamental toroidal standing Alfvén mode. These toroidal ULF pulsations with the regular sinusoidal waveforms displayed the approximately same periods as the whistler-mode power variations throughout the event. Along with the decay of the toroidal ULF pulsations, the whistler-mode quasiperiodic feature became indistinct. However, different from the situations in the previously reported compressional ULF modulation events (J. Li et al., 2017; W. Li et al., 2011; Xia et al., 2016), there were no observable modulation signatures of background parameters and resonant particles for the whistler-mode emissions in this specific event. From the available measurements, we speculate on the following as plausible explanations for this phenomenon: (1) The fundamental toroidal pulsations of magnetic field and plasma density had a node at the equator. (2) The hot electrons conserved the adiabatic invariants and exhibited physically little variations near the equator. The toroidal modulation of the geomagnetic field configuration caused the quasiperiodic variations in the nonlinear growth of chorus and in the propagation path of exohiss. (3) The hot protons were in bounce resonance with the toroidal ULF pulsations, producing the quasiperiodic variation in the linear growth of magnetosonic emissions. The satellite did not record the expected oscillations of hot proton fluxes because of the rapid relaxation or the limited detection efficiency. Future observational, theoretical, and numerical studies are required to examine the proposed scenarios.

Acknowledgments
We acknowledge Van Allen Probes teams for the use of data and acknowledge D. Summers for the helpful discussions at USTC. Data are available at the websites: http://emfisis.physics.uiowa.edu/Flight/ for EMFISIS and http://www.rbsp-ect.lanl.gov/data_pub/ for ECT. This work was supported by the National Natural Science Foundation of China grants 41774170 and 41631071, the Chinese Academy of Sciences grants KZCX2-EW-QN510 and KZZD-EW-01-4, the CAS Key Research Program of Frontier Sciences grant QYZDB-SSW-DQC015, the National Key Basic Research Special Foundation of China grant 2011CB811403, and the Key Research Program of the Chinese Academy of Sciences, grant XDPB11.

References

Anderson, B. J., Engebretson, M. J., Rounds, S. P., Zanetti, L. J., & Potemra, T. A. (1990). A statistical study of Pc 3–5 pulsations observed by the AMPTE/CCE magnetic fields experiment. I—Occurrence distributions. *Journal of Geophysical Research*, *95*, 10,495–10,523. https://doi.org/10.1029/JA095iA07p10495

Baker, D. N., Kanekal, S. G., Hoxie, V. C., Batiste, S., Bolton, M., Li, X., & Friedel, R. (2013). The Relativistic Electron-Proton Telescope (REPT) Instrument on board the Radiation Belt Storm Probes (RBSP) spacecraft: Characterization of Earth's eadiation belt high-energy particle populations. *Space Science Reviews*, *179*, 337–381. https://doi.org/10.1007/s11214-012-9950-9

Blake, J. B., Carranza, P. A., Claudepierre, S. G., Clemmons, J. H., Crain, W. R., Dotan, Y., & Zakrzewski, M. P. (2013). The Magnetic Electron Ion Spectrometer (MagEIS) Instruments aboard the Radiation Belt Storm Probes (RBSP) spacecraft. *Space Science Reviews*, *179*, 383–421. https://doi.org/10.1007/s11214-013-9991-8

Boardsen, S. A., Gallagher, D. L., Gurnett, D. A., Peterson, W. K., & Green, J. L. (1992). Funnel-shaped, low-frequency equatorial waves. *Journal of Geophysical Research*, *97*, 14,967–14,976. https://doi.org/10.1029/92JA00827

Boardsen, S. A., Hospodarsky, G. B., Kletzing, C. A., Pfaff, R. F., Kurth, W. S., Wygant, J. R., & MacDonald, E. A. (2014). Van Allen Probe observations of periodic rising frequencies of the fast magnetosonic mode. *Geophysical Research Letters*, *41*, 8161–8168. https://doi.org/10.1002/2014GL062020

Bortnik, J., Thorne, R. M., & Meredith, N. P. (2008). The unexpected origin of plasmaspheric hiss from discrete chorus emissions. *Nature*, *452*, 62–66. https://doi.org/10.1038/nature06741

Burtis, W. J., & Helliwell, R. A. (1975). Magnetospheric chorus—Amplitude and growth rate. *Journal of Geophysical Research*, *80*, 3265–3270. https://doi.org/10.1029/JA080i022p03265

Carson, W. B., Koch, J. A., Pope, J. H., & Gallet, R. M. (1965). Long-period very low frequency emission pulsations. *Journal of Geophysical Research*, *70*, 4293–4303. https://doi.org/10.1029/JZ070i017p04293

Claudepierre, S. G., Hudson, M. K., Lotko, W., Lyon, J. G., & Denton, R. E. (2010). Solar wind driving of magnetospheric ULF waves: Field line resonances driven by dynamic pressure fluctuations. *Journal of Geophysical Research*, *115*, A11202. https://doi.org/10.1029/2010JA015399

Coroniti, F. V., & Kennel, C. F. (1970). Electron precipitation pulsations. *Journal of Geophysical Research*, *75*(7), 1279–1289. https://doi.org/10.1029/JA075i007p01279

Davidson, G. T. (1979). Self-modulated VLF wave-electron interactions in the magnetosphere—A cause of auroral pulsations. *Journal of Geophysical Research*, *84*, 6517–6523. https://doi.org/10.1029/JA084iA11p06517

Davidson, G. T. (1986). Pitch angle diffusion in morningside aurorae 2. The formation of repetitive auroral pulsations. *Journal of Geophysical Research*, *91*, 4429–4436. https://doi.org/10.1029/JA091iA04p04429

Demekhov, A. G., & Trakhtengerts, V. Y. (1994). A mechanism of formation of pulsating aurorae. *Journal of Geophysical Research*, *99*, 5831–5841. https://doi.org/10.1029/93JA01804

Falkowski, B. J., Tsurutani, B. T., Lakhina, G. S., & Pickett, J. S. (2017). Two sources of dayside intense, quasi-coherent plasmaspheric hiss: A new mechanism for the slot region? *Journal of Geophysical Research: Space Physics*, *122*, 1643–1657. https://doi.org/10.1002/2016JA023289

Fu, H. S., Cao, J. B., Mozer, F. S., Lu, H. Y., & Yang, B. (2012). Chorus intensification in response to interplanetary shock. *Journal of Geophysical Research*, *117*, 1203. https://doi.org/10.1029/2011JA016913

Fu, H. S., Cao, J. B., Zhima, Z., Khotyaintsev, Y. V., Angelopoulos, V., Santolík, O., & Huang, S. Y. (2014). First observation of rising-tone magnetosonic waves. *Geophysical Research Letters*, *41*, 7419–7426. https://doi.org/10.1002/2014GL061867

Funsten, H. O., Skoug, R. M., Guthrie, A. A., MacDonald, E. A., Baldonado, J. R., Harper, R. W., & Chen, J. (2013). Helium, Oxygen, Proton, and Electron (HOPE) Mass Spectrometer for the Radiation Belt Storm Probes Mission. *Space Science Reviews*, *179*, 423–484. https://doi.org/10.1007/s11214-013-9968-7

Gao, Z., Su, Z., Xiao, F., Zheng, H., Wang, Y., Wang, S., & Funsten, H. O. (2018). Exohiss wave enhancement following substorm electron injection in the dayside magnetosphere. *Earth and Planetary Physics*, *2*(5), 359–370. https://doi.org/10.26464/epp2018033

Gary, S. P., Liu, K., Winske, D., & Denton, R. E. (2010). Ion Bernstein instability in the terrestrial magnetosphere: Linear dispersion theory. *Journal of Geophysical Research*, *115*, A12209. https://doi.org/10.1029/2010JA015965

Gulelmi, A. V., Klaine, B. I., & Potapov, A. S. (1975). Excitation of magnetosonic waves with discrete spectrum in the equatorial vicinity of the plasmapause. *Planetary and Space Science*, *23*, 279–286. https://doi.org/10.1016/0032-0633(75)90133-6

Gurnett, D. A. (1976). Plasma wave interactions with energetic ions near the magnetic equator. *Journal of Geophysical Research*, *81*, 2765–2770. https://doi.org/10.1029/JA081i016p02765

Hayakawa, M., & Sazhin, S. S. (1992). Mid-latitude and plasmaspheric hiss—A review. *Planetary and Space Science*, *40*, 1325–1338. https://doi.org/10.1016/0032-0633(92)90089-7

Helliwell, R. A. (1965). *Whistlers and related ionospheric phenomena*. Stanford, CA: Stanford University Press.

Horne, R. B., & Thorne, R. M. (1998). Potential waves for relativistic electron scattering and stochastic acceleration during magnetic storms. *Geophysical Research Letters*, *25*, 3011–3014. https://doi.org/10.1029/98GL01002

Hudson, M., Denton, R., Lessard, M., Miftakhova, E., & Anderson, R. (2004). A study of Pc-5 ULF oscillations. *Annales Geophysicae*, *22*, 289–302. https://doi.org/10.5194/angeo-22-289-2004

Jaynes, A. N., Lessard, M. R., Takahashi, K., Ali, A. F., Malaspina, D. M., Michell, R. G., & Wygant, J. R. (2015). Correlated Pc4-5 ULF waves, whistler-mode chorus, and pulsating aurora observed by the Van Allen Probes and ground-based systems. *Journal of Geophysical Research: Space Physics*, *120*, 8749–8761. https://doi.org/10.1002/2015JA021380

Katoh, Y., & Omura, Y. (2013). Effect of the background magnetic field inhomogeneity on generation processes of whistler-mode chorus and broadband hiss-like emissions. *Journal of Geophysical Research: Space Physics*, *118*, 4189–4198. https://doi.org/10.1002/jgra.50395

Katoh, Y., Omura, Y., Miyake, Y., Usui, H., & Nakashima, H. (2018). Dependence of generation of whistler mode chorus emissions on the temperature anisotropy and density of energetic electrons in the Earth's inner magnetosphere. *Journal of Geophysical Research: Space Physics*, *123*, 1165–1177. https://doi.org/10.1002/2017JA024801

Keika, K., Spasojevic, M., Li, W., Bortnik, J., Miyoshi, Y., & Angelopoulos, V. (2012). PENGUIn/AGO and THEMIS conjugate observations of whistler mode chorus waves in the dayside uniform zone under steady solar wind and quiet geomagnetic conditions. *Journal of Geophysical Research*, *117*, A07212. https://doi.org/10.1029/2012JA017708

Kim, K. C., & Chen, L. (2016). Modeling the storm time behavior of the magnetosonic waves using solar wind parameters. *Journal of Geophysical Research: Space Physics*, *121*, 446–458. https://doi.org/10.1002/2015JA021716

Kimura, I. (1974). Interrelation between VLF and ULF Emissions. *Space Science Reviews*, *16*, 389–411. https://doi.org/10.1007/BF00171565

Kitamura, T., Jacobs, J. A., Watanabe, T., & Flint, R. B. (1969). An investigation of quasi-periodic VLF emissions. *Journal of Geophysical Research*, *74*(24), 5652–5664. https://doi.org/10.1029/JA074i024p05652

Kletzing, C. A., Kurth, W. S., Acuna, M., MacDowall, R. J., Torbert, R. B., Averkamp, T., & Tyler, J. (2013). The Electric and Magnetic Field Instrument Suite and Integrated Science (EMFISIS) on RBSP. *Space Science Reviews*, *179*, 127–181. https://doi.org/10.1007/s11214-013-9993-6

Kurth, W. S., Pascuale, S. D., Faden, J. B., Kletzing, C. A., Hospodarsky, G. B., Thaller, S., & Wygant, J. R. (2014). Electron densities inferred from plasma wave spectra obtained by the waves instrument on Van Allen Probes. *Journal of Geophysical Research: Space Physics*, *120*, 904–914. https://doi.org/10.1002/2014JA020857

Li, J., Bortnik, J., Li, W., Thorne, R. M., Ma, Q., Chu, X., & Thaller, S. (2017). Coherently modulated whistler mode waves simultaneously observed over unexpectedly large spatial scales. *Journal of Geophysical Research: Space Physics*, *122*, 1871–1882. https://doi.org/10.1002/2016JA023706

Li, W., Chen, L., Bortnik, J., Thorne, R. M., Angelopoulos, V., Kletzing, C. A., & Hospodarsky, G. B. (2015). First evidence for chorus at a large geocentric distance as a source of plasmaspheric hiss: Coordinated THEMIS and Van Allen Probes observation. *Geophysical Research Letters*, *42*, 241–248. https://doi.org/10.1002/2014GL062832

Li, W., Thorne, R. M., Angelopoulos, V., Bortnik, J., Cully, C. M., Ni, B., & Magnes, W. (2009). Global distribution of whistler-mode chorus waves observed on the THEMIS spacecraft. *Geophysical Research Letters*, *36*, L09104. https://doi.org/10.1029/2009GL037595

Li, W., Thorne, R. M., Bortnik, J., Nishimura, Y., & Angelopoulos, V. (2011). Modulation of whistler mode chorus waves: 1. Role of compressional Pc4–5 pulsations. *Journal of Geophysical Research*, *116*, A6205. Retrieved from http://doi.wiley.com/10.1029/2010JA016313 https://doi.org/10.1029/2010JA016312

Liu, N., Su, Z., Gao, Z., Reeves, G. D., Zheng, H., Wang, Y., & Wang, S. (2017). Shock-induced disappearance and subsequent recovery of plasmaspheric hiss: Coordinated observations of RBSP, THEMIS, and POES Satellites. *Journal of Geophysical Research: Space Physics*, *122*, 10,421–10,435. https://doi.org/10.1002/2017JA024470

Liu, N., Su, Z., Gao, Z., Zheng, H., Wang, Y., Wang, S., & Wygant, J. R. (2017). Simultaneous disappearances of plasmaspheric hiss, exohiss, and chorus waves triggered by a sudden decrease in solar wind dynamic pressure. *Geophysical Research Letters*, *44*, 52–61. https://doi.org/10.1002/2016GL071987

Liu, N., Su, Z., Zheng, H., Wang, Y., & Wang, S. (2018a). Magnetosonic harmonic falling and rising frequency emissions potentially generated by nonlinear wave-wave interactions in the Van Allen Radiation Belts. *Geophysical Research Letters*, *45*, 7985–7995. https://doi.org/10.1029/2018GL079232

Liu, N., Su, Z., Zheng, H., Wang, Y., & Wang, S. (2018b). Prompt disappearance and emergence of radiation belt magnetosonic waves induced by solar wind dynamic pressure variations. *Geophysical Research Letters*, *45*, 585–594. https://doi.org/10.1002/2017GL076382

Ma, Q., Li, W., Thorne, R. M., & Angelopoulos, V. (2013). Global distribution of equatorial magnetosonic waves observed by THEMIS. *Geophysical Research Letters*, *40*, 1895–1901. https://doi.org/10.1002/grl.50434

Malaspina, D. M., Jaynes, A. N., Boulé, C., Bortnik, J., Thaller, S. A., Ergun, R. E., & Wygant, J. R. (2016). The distribution of plasmaspheric hiss wave power with respect to plasmapause location. *Geophysical Research Letters*, *43*, 7878–7886. https://doi.org/10.1002/2016GL069982

Manninen, J., Kleimenova, N. G., Kozyreva, O. V., & Turunen, T. (2010). Pc5 geomagnetic pulsations, pulsating particle precipitation, and VLF chorus: Case study on 24 November 2006. *Journal of Geophysical Research*, *115*, A00F14. https://doi.org/10.1029/2009JA014837

Mauk, B. H., Fox, N. J., Kanekal, S. G., Kessel, R. L., Sibeck, D. G., & Ukhorskiy, A. (2013). Science objectives and rationale for the Radiation Belt Storm Probes Mission. *Space Science Reviews*, *179*, 3–27. https://doi.org/10.1007/s11214-012-9908-y

McPherron, R. L., Parks, G. K., Coroniti, F. V., & Ward, S. H. (1968). Studies of the magnetospheric substorm: 2. Correlated magnetic micropulsations and electron precipitation occurring during auroral substorms. *Journal of Geophysical Research*, *73*(5), 1697–1713. https://doi.org/10.1029/JA073i005p01697

Meredith, N. P., Horne, R. B., & Anderson, R. R. (2001). Substorm dependence of chorus amplitudes: Implications for the acceleration of electrons to relativistic energies. *Journal of Geophysical Research*, *106*, 13,165–13,178. https://doi.org/10.1029/2000JA900156

Meredith, N. P., Horne, R. B., Thorne, R. M., Summers, D., & Anderson, R. R. (2004). Substorm dependence of plasmaspheric hiss. *Journal of Geophysical Research*, *109*, A06209. https://doi.org/10.1029/2004JA010387

Němec, F., Pickett, J. S., & Santolík, O. (2014). Multispacecraft Cluster observations of quasiperiodic emissions close to the geomagnetic equator. *Journal of Geophysical Research: Space Physics*, *119*, 9101–9112. https://doi.org/10.1002/2014JA020321

Němec, F., Santolík, O., Hrbáčková, Z., Pickett, J. S., & Cornilleau-Wehrlin, N. (2015). Equatorial noise emissions with quasiperiodic modulation of wave intensity. *Journal of Geophysical Research: Space Physics*, *120*, 2649–2661. https://doi.org/10.1002/2014JA020816

Omura, Y., Katoh, Y., & Summers, D. (2008). Theory and simulation of the generation of whistler-mode chorus. *Journal of Geophysical Research*, *113*, 4223. https://doi.org/10.1029/2007JA012622

Pasmanik, D., Demekhov, A., Trakhtengerts, V., & Parrot, M. (2004). Modeling whistler wave generation regimes in magnetospheric cyclotron maser. *Annales Geophysicae*, *22*, 3561–3570. https://doi.org/10.5194/angeo-22-3561-2004

Pasmanik, D., Titova, E., Demekhov, A., Trakhtengerts, V., Santolik, O., Jiricek, F., & Parrot, M. (2004). Quasi-periodic ELF/VLF wave emissions in the Earth's magnetosphere: Comparison of satellite observations and modeling. *Annales Geophysicae*, *22*, 4351–4361. https://doi.org/10.5194/angeo-22-4351-2004

Perraut, S., Roux, A., Robert, P., Gendrin, R., Sauvaud, J. A., Bosqued, J. M., & Korth, A. (1982). A systematic study of ULF waves above F_{H^+} from GEOS 1 and 2 measurements and their relationships with proton ring distributions. *Journal of Geophysical Research*, *87*, 6219–6236. https://doi.org/10.1029/JA087iA08p06219

Rae, I. J., Mann, I. R., Murphy, K. R., Ozeke, L. G., Milling, D. K., Chan, A. A., & Honary, F. (2012). Ground-based magnetometer determination of in situ Pc4–5 ULF electric field wave spectra as a function of solar wind speed. *Journal of Geophysical Research*, *117*, A04221. https://doi.org/10.1029/2011JA017335

Russell, C. T., Holzer, R. E., & Smith, E. J. (1969). OGO 3 observations of ELF noise in the magnetosphere. 1. Spatial extent and frequency of occurrence. *Journal of Geophysical Research*, *74*, 755–777. https://doi.org/10.1029/JA074i003p00755

Russell, C. T., Holzer, R. E., & Smith, E. J. (1970). OGO 3 observations of ELF noise in the magnetosphere. 2. The nature of the equatorial noise. *Journal of Geophysical Research*, *75*, 755–768. https://doi.org/10.1029/JA075i004p00755

Santolík, O., Parrot, M., & Lefeuvre, F. (2003). Singular value decomposition methods for wave propagation analysis. *Radio Science*, *38*(1), 1010. https://doi.org/10.1029/2000RS002523

Santolík, O., Pickett, J. S., Gurnett, D. A., Menietti, J. D., Tsurutani, B. T., & Verkhoglyadova, O. (2010). Survey of Poynting flux of whistler mode chorus in the outer zone. *Journal of Geophysical Research*, *115*, A00F13. https://doi.org/10.1029/2009JA014925

Santolík, O., Pickett, J. S., Gurnett, D. A., & Storey, L. R. O. (2002). Magnetic component of narrowband ion cyclotron waves in the auroral zone. *Journal of Geophysical Research*, *107*, 1444. https://doi.org/10.1029/2001JA000146

Sato, N., & Fukunishi, H. (1981). Interaction between ELF-VLF emissions and magnetic pulsations: Classification of quasi-periodic emissions based on frequency-time spectra. *Journal of Geophysical Research*, *86*, 19–29. https://doi.org/10.1029/JA086iA01p00019

Sato, N., Hayashi, K., Kokubun, S., Oguti, T., & Fukunishi, H. (1974). Relationships between quasi-periodic VLF emission and geomagnetic pulsation. *Journal of Atmospheric and Terrestrial Physics*, *36*, 1515–1526. https://doi.org/10.1016/0021-9169(74)90229-3

Sato, N., & Kokubun, S. (1980). Interaction between ELF-VLF emissions and magnetic pulsations—Quasi-periodic ELF-VLF emissions associated with Pc3–4 magnetic pulsations and their geomagnetic conjugacy. *Journal of Geophysical Research*, *85*, 101–113. https://doi.org/10.1029/JA085iA01p00101

Shprits, Y. Y. (2009). Potential waves for pitch-angle scattering of near-equatorially mirroring energetic electrons due to the violation of the second adiabatic invariant. *Geophysical Research Letters*, *36*, L12106. https://doi.org/10.1029/2009GL038322

Shprits, Y. Y., Runov, A., & Ni, B. (2013). Gyro-resonant scattering of radiation belt electrons during the solar minimum by fast magnetosonic waves. *Journal of Geophysical Research: Space Physics*, *118*, 648–652. https://doi.org/10.1002/jgra.50108

Southwood, D. J., & Kivelson, M. G. (1981). Charged particle behavior in low-frequency geomagnetic pulsations. I. Transverse waves. *Journal of Geophysical Research*, *86*, 5643–5655. https://doi.org/10.1029/JA086iA07p05643

Southwood, D. J., & Kivelson, M. G. (1982). Charged particle behavior in low-frequency geomagnetic pulsations. II—Graphical approach. *Journal of Geophysical Research*, *87*, 1707–1710. https://doi.org/10.1029/JA087iA03p01707

Spence, H. E., Reeves, G. D., Baker, D. N., Blake, J. B., Bolton, M., Bourdarie, S., & Thorne, R. M. (2013). Science Goals and Overview of the Energetic Particle, Composition, and Thermal Plasma (ECT) Suite on NASAs Radiation Belt Storm Probes (RBSP) Mission. *Space Science Reviews*, *179*, 311–336. https://doi.org/10.1007/s11214-013-0007-5

Su, Z., Liu, N., Zheng, H., Wang, Y., & Wang, S. (2018a). Large-amplitude extremely low frequency hiss waves in plasmaspheric plumes. *Geophysical Research Letters*, *45*, 565–577. https://doi.org/10.1002/2017GL076754

Su, Z., Liu, N., Zheng, H., Wang, Y., & Wang, S. (2018b). Multipoint observations of nightside plasmaspheric hiss generated by substorm-injected electrons. *Geophysical Research Letters*, *45*, 10,921–10,932. https://doi.org/10 10.1029/2018GL079927

Su, Z., Wang, G., Liu, N., Zheng, H., Wang, Y., & Wang, S. (2017). Direct observation of generation and propagation of magnetosonic waves following substorm injection. *Geophysical Research Letters*, *44*, 7587–7597. https://doi.org/10.1002/2017GL074362

Su, Z., Zhu, H., Xiao, F., Zheng, H., Wang, Y., He, Z., & Wygant, J. R. (2014). Intense duskside lower band chorus waves observed by Van Allen Probes: Generation and potential acceleration effect on radiation belt electrons. *Journal of Geophysical Research: Space Physics*, *119*, 4266–4273. https://doi.org/10.1002/2014JA019919

Su, Z., Zhu, H., Xiao, F., Zheng, H., Wang, Y., Shen, C., & Wygant, J. R. (2015). Disappearance of plasmaspheric hiss following interplanetary shock. *Geophysical Research Letters*, *42*, 3129–3140. https://doi.org/10.1002/2015GL063906

Su, Z., Zhu, H., Xiao, F., Zong, Q. G., Zhou, X. Z., Zheng, H., & Wygant, J. R. (2015). Ultra-low-frequency wave-driven diffusion of radiation belt relativistic electrons. *Nature Communication*, *6*, 10096. https://doi.org/10.1038/ncomms10096

Summers, D., Ni, B., & Meredith, N. P. (2007). Timescales for radiation belt electron acceleration and loss due to resonant wave-particle interactions: 1. Theory. *Journal of Geophysical Research*, *112*, A04206. https://doi.org/10.1029/2006JA011801

Summers, D., Thorne, R. M., & Xiao, F. (1998). Relativistic theory of wave-particle resonant diffusion with application to electron acceleration in the magnetosphere. *Journal of Geophysical Research*, *103*, 20487. https://doi.org/10.1029/98JA01740

Takahashi, K., Denton, R. E., Anderson, R. R., & Hughes, W. J. (2006). Mass density inferred from toroidal wave frequencies and its comparison to electron density. *Journal of Geophysical Research*, *111*, A01201. https://doi.org/10.1029/2005JA011286

Thorne, R. M. (2010). Radiation belt dynamics: The importance of wave-particle interactions. *Geophysical Research Letters*, *37*, L22107. https://doi.org/10.1029/2010GL044990

Thorne, R. M., Church, S. R., & Gorney, D. J. (1979). On the origin of plasmaspheric hiss—The importance of wave propagation and the plasmapause. *Journal of Geophysical Research*, *84*. https://doi.org/5241-5247 10.1029/JA084iA09p05241

Thorne, R. M., Smith, E. J., Burton, R. K., & Holzer, R. E. (1973). Plasmaspheric hiss. *Journal of Geophysical Research*, *78*, 1581–1596. https://doi.org/10.1029/JA078i010p01581

Titova, E. E., Kozelov, B. V., Demekhov, A. G., Manninen, J., Santolik, O., Kletzing, C. A., & Reeves, G. (2015). Identification of the source of quasiperiodic VLF emissions using ground-based and Van Allen Probes satellite observations. *Geophysical Research Letters*, *42*, 6137–6145. https://doi.org/10.1002/2015GL064911

Tixier, M., & Cornilleau-Wehrlin, N. (1986). How are the VLF quasi-periodic emissions controlled by harmonics of field line oscillations?—The results of a comparison between ground and GEOS satellites measurements. *Journal of Geophysical Research*, *91*, 6899–6919. https://doi.org/10.1029/JA091iA06p06899

Trakhtengerts, V. Y. (1995). Magnetosphere cyclotron maser: Backward wave oscillator generation regime. *Journal of Geophysical Research*, *100*, 17,205–17,210. https://doi.org/10.1029/95JA00843

Tsurutani, B. T., Falkowski, B. J., Pickett, J. S., Santolik, O., & Lakhina, G. S. (2015). Plasmaspheric hiss properties: Observations from Polar. *Journal of Geophysical Research: Space Physics*, *120*, 414–431. https://doi.org/10.1002/2014JA020518

Tsurutani, B. T., Falkowski, B. J., Pickett, J. S., Verkhoglyadova, O. P., Santolik, O., & Lakhina, G. S. (2014). Extremely intense ELF magnetosonic waves: A survey of polar observations. *Journal of Geophysical Research: Space Physics*, *119*, 964–977. https://doi.org/10.1002/2013JA019284

Tsurutani, B. T., Park, S. A., Falkowski, B. J., Lakhina, G. S., Pickett, J. S., Bortnik, J., et al. (2018). Plasmaspheric hiss: Coherent and intense. *Journal of Geophysical Research: Space Physics*, *123*, 10,009–10,029. https://doi.org/10.1029/2018JA025975

Tsurutani, B. T., & Smith, E. J. (1974). Postmidnight chorus: A substorm phenomenon. *Journal of Geophysical Research*, *79*(1), 118–127. https://doi.org/10.1029/JA079i001p00118

Tsurutani, B. T., & Smith, E. J. (1977). Two types of magnetospheric ELF chorus and their substorm dependences. *Journal of Geophysical Research*, *82*, 5112–5128. https://doi.org/10.1029/JA082i032p05112

Tsurutani, B. T., Smith, E. J., West, H. I., & Buck, R. M. (1979). Chorus, energetic electrons and magnetospheric substorms. In P. J. Palmadesso & K. Papadopoulos (Eds.), *Wave instabilities in space plasmas* (pp. 55–62). Dordrecht, Netherlands: Springer.

Tsurutani, B. T., Verkhoglyadova, O. P., Lakhina, G. S., & Yagitani, S. (2009). Properties of dayside outer zone chorus during HILDCAA events: Loss of energetic electrons. *Journal of Geophysical Research*, *114*, A03207. https://doi.org/10.1029/2008JA013353

Tsyganenko, N. A., & Sitnov, M. I. (2005). Modeling the dynamics of the inner magnetosphere during strong geomagnetic storms. *Journal of Geophysical Research*, *110*, A03208. https://doi.org/10.1029/2004JA010798

Walker, S. N., Demekhov, A. G., Boardsen, S. A., Ganushkina, N. Y., Sibeck, D. G., & Balikhin, M. A. (2016). Cluster observations of non-time continuous magnetosonic waves. *Journal of Geophysical Research: Space Physics*, *121*, 9701–9716. https://doi.org/10.1002/2016JA023287

Watt, C. E. J., Degeling, A. W., Rankin, R., Murphy, K. R., Rae, I. J., & Singer, H. J. (2011). Ultralow-frequency modulation of whistler-mode wave growth. *Journal of Geophysical Research*, *116*, A10209. https://doi.org/10.1029/2011JA016730

Wygant, J., Bonnell, J., Goetz, K., Ergun, R., Mozer, F., Bale, S., & Tao, J. (2013). The electric field and waves instruments on the Radiation Belt Storm Probes Mission. *Space Science Reviews*, *179*(1–4), 183–220. https://doi.org/10.1007/s11214-013-0013-7

Xia, Z., Chen, L., Dai, L., Claudepierre, S. G., Chan, A. A., Soto-Chavez, A., & Reeves, G. (2016). Modulation of chorus intensity by ULF waves deep in the inner magnetosphere. *Geophysical Research Letters*, *43*, 9444–9452. https://doi.org/10.1002/2016GL070280

Yang, B., Zong, Q. G., Wang, Y. F., Fu, S. Y., Song, P., Fu, H. S., & Reme, H. (2010). Cluster observations of simultaneous resonant interactions of ULF waves with energetic electrons and thermal ion species in the inner magnetosphere. *Journal of Geophysical Research*, *115*. https://doi.org/A02214 10.1029/2009JA014542

Zhu, H., Su, Z., Xiao, F., Zheng, H., Wang, Y., Shen, C., et al. (2015). Plasmatrough exohiss waves observed by Van Allen Probes: Evidence for leakage from plasmasphere and resonant scattering of radiation belt electrons. *Geophysical Research Letters*, *42*, 1012–1019. https://doi.org/10.1002/2014GL062964